Phage Display on the Anti-infective Target 1-Deoxy-D-xylulose-5-phosphate Synthase Leads to an Acceptor–Substrate Competitive Peptidic Inhibitor

Alessio Marcozzi+,[a] Tiziana Masini+,[b] Di Zhu+,[b, c] Diego Pesce,[a] Boris Illarionov,[d] Markus Fischer,[d] Andreas Herrmann,*[a] and Anna K. H. Hirsch*[b, c, e]

Enzymes of the 2-C-methyl-D-erythritol-4-phosphate pathway for the biosynthesis of isoprenoid precursors are validated drug targets. By performing phage display on 1-deoxy-D-xylulose-5-phosphate synthase (DXS), which catalyzes the first step of this pathway, we discovered several peptide hits and recognized false-positive hits. The enriched peptide binder P12 emerged as a substrate (D-glyceraldehyde-3-phosphate)-competitive inhibitor of Deinococcus radiodurans DXS. The results indicate possible overlap of the cofactor- and acceptor-substrate-binding pockets and provide inspiration for the design of inhibitors of DXS with a unique and novel mechanism of inhibition.

Introduction

Bacterial and protozoan infections are widely spread in some human populations. The main burden of malaria and tuberculosis lies in resource-poor countries, for which, for example, co-infection with human immunodeficiency virus (HIV) can dramatically increase the mortality rate.[1,2] Moreover, in these countries, drug compliance is often incomplete; this leads to the emergence of drug-resistant strains of the pathogens, against which most of the available drugs are no longer effec-

tive. Therefore, there is an urgent need for the discovery of drugs with novel mechanisms of action that are able to overcome the issue of drug resistance.[3]

The enzymes of the 2-C-methyl-D-erythritol-4-phosphate (MEP, 1) pathway for the biosynthesis of the essential isoprenoid precursors isopentenyl diphosphate (2) and dimethylallyl diphosphate (3) have been studied over the past decade as potential targets for the development of antimalarial and anti-tuberculotic drugs (Scheme 1A).[4] The particular interest of medicinal chemists in these enzymes arises from the fact that the MEP pathway has been genetically validated as essential in multiple organisms, including Mycobacterium tuberculosis[5] and Plasmodium falciparum,[6] causative agents of tuberculosis and malaria, respectively, but is absent in humans,[7,8] who exclusively utilize the alternative mevalonate pathway for the biosynthesis of 2 and 3.[9] This distinct taxonomic distribution sets the stage for the development of selective drugs targeting the enzymes of the MEP pathway.[10] An increasing number of inhibitors for the enzymes of the MEP pathway have been published, especially thanks to the growing number of crystal and co-crystal structures deposited in the RCSB Protein Data Bank,[11] with fosmidomycin—an inhibitor of the second enzyme of the pathway IspC—being the most successful example to date, given that it is the only inhibitor of the MEP pathway that is being investigated clinically, in combination with piperaquine.[12]

One of the least studied among the enzymes of the MEP pathway is 1-deoxy-D-xylulose-5-phosphate synthase (DXS), which catalyzes the first and rate-limiting steps of the MEP pathway, consisting in the thiamine-diphosphate (ThDP)-dependent decarboxylative condensation of pyruvate (4) and D-glyceraldehyde-3-phosphate (5) to afford 1-deoxy-D-xylulose-5-phosphate (6). Despite the high degree of sequence homology of the ThDP-binding site of DXS with other human ThDP-dependent enzymes [e.g., transketolase (TK) or pyruvate dehy-

[a] Dr. A. Marcozzi,+ Dr. D. Pesce, Prof. Dr. A. Herrmann
Department Zernike Institute for Advanced Materials
University of Groningen
Nijenborgh 4, 9747 AG, Groningen (The Netherlands)
E-mail: a.herrmann@rug.nl

[b] Dr. T. Masini,+ D. Zhu,+ Prof. Dr. A. K. H. Hirsch
Stratingh Institute for Chemistry, University of Groningen
Nijenborgh 7, 9747 AG, Groningen (The Netherlands)

[c] D. Zhu,+ Prof. Dr. A. K. H. Hirsch
Helmholtz Institute for Pharmaceutical Research Saarland (HIPS)
Helmholtz Centre for Infection Research (HZI)
Department of Drug Design and Optimization
Campus Building E8.1, 66123 Saarbrücken (Germany)
E-mail: anna.hirsch@helmholtz-hzi.de

[d] Dr. B. Illarionov, Prof. Dr. M. Fischer
Hamburg School of Food Science, Institute of Food Chemistry
Grindelallee 117, 20146, Hamburg (Germany)

[e] Prof. Dr. A. K. H. Hirsch
Department of Pharmacy, Medicinal Chemistry, Saarland University
Campus Building E8.1, 66123 Saarbrücken (Germany)

[+] These authors contributed equally to this work. This is contribution 189 from the Institute to Reduce the Incidence of Nosocomial Infections.

Supporting Information and the ORCID identification numbers for the authors of this article can be found under https://doi.org/10.1002/cbic.201700402.
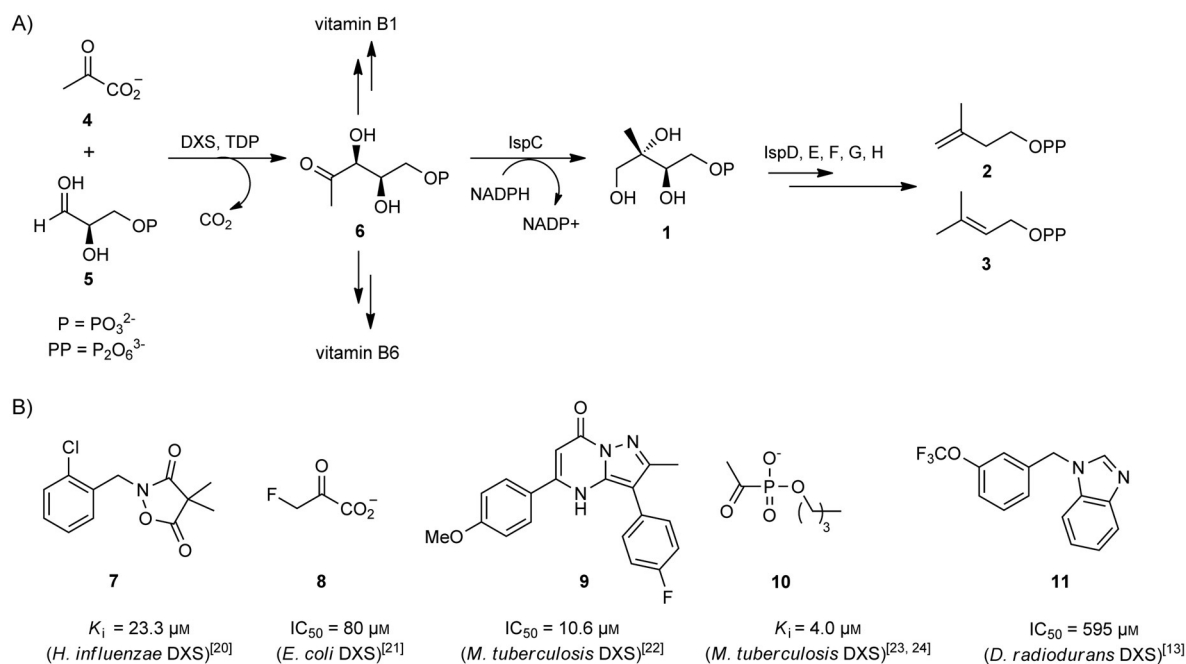
Scheme 1. Overview of the MEP pathway. A) 2-*C*-methyl-D-erythritol-4-phosphate (MEP, **1**) pathway for the synthesis of isopentenyl diphosphate (**2**) and dimethylallyl diphosphate (**3**), universal precursors for the biosynthesis of isoprenoids. B) Selection of known inhibitors of DXS (**7**–**11**).

drogenase (PDH); for TK: 20% sequence identity overall, 47% sequence identity in the ThDP-binding pocket between *M. tuberculosis* DXS and human TK],[13] DXS has distinctive features compared to mammalian ThDP-dependent enzymes, from both structural and kinetic points of view. In fact, together with the peculiar domain arrangement, in which the particularly big ThDP-binding site is located within the same monomer,[14] DXS has a unique catalytic mechanism that involves the formation of a ternary complex with substrates **4** and **5**,[15] whereas all other ThDP-dependent enzymes follow classical ping-pong kinetics.[16] By taking advantage of these distinctive features, selective inhibition of DXS over human ThDP-dependent enzymes should be possible. The potential of DXS as a drug target is also underlined by its involvement in pyridoxal phosphate (vitamin B6)[17] and thiamine (vitamin B1)[18] biosynthesis in many bacteria, offering the opportunity to target three metabolic pathways at once. Furthermore, DXS possesses an important regulatory role for the flux of metabolites throughout the whole MEP pathway as shown recently.[19]

Considering its crucial importance in bacterial metabolism, it is surprising that DXS is one of the least studied among the enzymes of the MEP pathway in terms of crystallography and inhibitor development. In fact, there are just two crystal structures deposited in the PDB of the enzyme in complex with its cofactor ThDP (*Escherichia coli*, PDB ID: 2O1S, incomplete crystal structure; *Deinococcus radiodurans*, PDB ID: 2O1X).[14] The amino-acid residues lining the ThDP-binding pocket are highly conserved among the DXS enzymes in different organisms (e.g., 68% sequence identity in the ThDP-binding pocket and 38% sequence identity overall between *D. radiodurans* and *M. tuberculosis* DXS). However, striking differences in inhibitory potency or affinity have been observed upon evaluating ThDP-

competitive inhibitors against distinct orthologues.[20] The herbicide ketoclomazone, for which no information about the mode of inhibition (MOI) is available, is known to weakly inhibit *Chlamydomonas* DXS (IC$_{50}$ = 0.1 mM),[21] whereas it is significantly more potent against *Haemophilus influenzae* DXS (K_i = 23 μM).[22] Moreover, the number of inhibitors for DXS reported in the literature to date (e.g., **7**–**11**, Scheme 1B) is very limited, as is the structural information about the corresponding binding modes.[4, 22–26] Phosphonates such as **10** have been shown to be pyruvate-competitive inhibitors, with K_i values in the low micromolar range against *M. tuberculosis* DXS and remarkable selectivity over mammalian ThDP-dependent enzymes.[25, 26] We recently reported fragment **11** to be a moderate inhibitor of *D. radiodurans* DXS (IC$_{50}$ = 595 μM) and validated its binding mode in solution by using a combination of NMR spectroscopy techniques.[13]

All the inhibitors for DXS reported in the literature so far are small, organic molecules, but to our knowledge, there is no report on peptidic inhibitors. Even though peptides still partially suffer from a "deficit in image", most of the limits associated with their development and optimization as therapeutic agents have been overcome in the past decade. The fact that peptides have several advantages over small organic molecules encouraged medicinal chemists to reconsider their potential as drug candidates. For example, the risk of systemic toxicity associated with their administration is reduced, and thanks to their short half-life, they do not tend to accumulate in tissues, with a reduced risk of complications caused by their metabolites.[27] In addition, they offer the advantage that they can be effectively selected to bind functional sites of target enzymes with high specificity.[28, 29] Moreover, multiple peptides can be used to target different parts of the same enzyme, thus lead-

ing to a decrease in activity by binding to the active or allosteric regulatory sites or by altering its surface properties.[30,31] Similar with other ThDP-dependent enzymes,[32,33] binding of ThDP with DXS is very tight ($K_d = 0.114$ μM for *Deinococcus radiodurans*; $K_d = 3.1$ μM for *M. tuberculosis*).[13] The large active site and high binding affinity for ThDP make it attractive to develop ThDP-competitive peptidic inhibitors.

Combinatorial peptide libraries have been used as a source of ligands for a variety of macromolecules, and different methods are known to select high-affinity binders from such libraries. One of the most efficient and cost-effective methods to select peptide binders is phage display (Figure S1 in the Supporting Information).[34] By using this technique, random peptides can be expressed on the surface of a bacteriophage leading to libraries with a complexity of up to 10^9 different peptides, which are subjected to several rounds of selection by which only target-bound phages are retained. The use of phage display allows large libraries of potential inhibitors to be screened without the need for a classical high-throughput screening (HTS) campaign or chemical synthesis of large libraries.

Results and Discussion

To identify peptidic inhibitors for DXS, we chose to exploit phage display by using the model enzyme *D. radiodurans* DXS, given that it is more stable than *M. tuberculosis* DXS.

We checked the stability of *D. radiodurans* DXS both at 4 °C and at room temperature by monitoring its activity for up to 37 h by using IspC as an auxiliary enzyme, which enables spectrophotometric monitoring of the consumption of NADPH. No loss in activity was observed even after 37 h at room temperature. From these initial tests, we concluded that *D. radiodurans* DXS was stable enough to be used as a target during the phage-display process. To rule out that we select for support binders, we designed a phage-display protocol for which the phages were incubated in solution with DXS, and DXS was subsequently recovered by affinity purification by using magnetic beads. We used a two-step selection approach to identify peptide binders (Table 1). During the first step, we screened a fully random M13 bacteriophage peptide library to detect specific sequences that are able to bind any part of the surface of

DXS. During this step, we used two types of magnetic beads and several elution buffers to avoid background-selection bias (Figure S2). Analysis of the selected peptides enabled us to design a new and more stringent library for the second selection step, in which we screened for sequences that could specifically bind to the ThDP-binding site of DXS. We used a solution of ThDP as competitive eluent to select only phages that interact at the ThDP-binding site. Given that unspecific binders are often present after the second round of selection, we added wild-type M13 phages as competitors: wild-type phages efficiently compete with virus particles expressing the peptide library for unspecific phage-target interactions, and they can be easily filtered out during postsequencing analysis. Both measures decrease the probability of selecting unspecific binders or false positives.

We used a commercially available M13 library PhD12 (NEB E8111L) for the first phage-display selection against DXS. After three rounds of selection, the analysis of the sequences clearly showed that a true selection had occurred: several sequences were repeated multiple times; this indicated their enrichment in the population (Table 2). Moreover, we observed an increase in the phage titer during the selection. Even though no clear motif emerged, we decided to test the most recurrent peptides to investigate their effect on DXS.

We took the four most prevalent sequences (i.e., **P1**–**P4**, Table 2) and tested the synthesized peptides for their inhibito-

Table 1. Overview of the two phage-display protocols used for the first and second selections.

	Phage display I	Phage display II
library	X₁₂GGGS	XSSX₉GGGS
competitors	none	wild-type M13
Rounds I and II		
target	desthiobiotin-DXS	His-tag-DXS
solid support	streptavidin-coated beads	nickel-coated beads
eluent	biotin	ThDP
Round III		
target	His-tag-DXS	not performed
solid support	nickel-coated beads	not performed
eluent	imidazole	not performed

Table 2. List of amino-acid sequences obtained after the first round of phage display.

Sequence ID[a]	Sequence[b]	Peptide ID[c,d]
07AJ42	VNHEYKLHSIKY	
07AJ43	TAELYPDLQSSQ	**P2** (×2)
07AJ47	DDTYPSRPVYLK	
07AJ52	DLYLSHGAPPQH	
07AJ53	HVTHNITNESNS	
07AJ55	ARMTFSQMSPHT	
07AJ59	TGSIRPKLHASP	
07AJ60	MSSRSRPHINSL	**P3** (×3)
07AJ61	QLARMSSLHVPM	
07AJ63	EDARRPPTSTEH	**P4** (×2)
07AJ64	SHEISRITAVSK	
07AJ67	VDMVTKQLLEYP	
07AJ68	ELQIGSWRMPPM	
06DB70	SERLMTPPKLFR	
07AJ71	MTHKQMHKHHGL	
07AJ72	LVSLTPPWINVD	
07AJ73	SSAQMNLNTFLN	**P13**
06DB52	PVNKQHTSLQNN	**P1** (×2)
06DB54	LGSHNIRLGEGS	
06DB58	YPHPIRQNFFAY	
06DB61	KSHTENSFTNVW	
06DB62	KLPPMNSDSMVW	
06DB68	HMNAHLTFQSAI	
06DB69	DAVKTHHLKHHS	

[a] Sequencing file identification number. [b] Peptide sequences were generated by translating the sequenced DNA considering the "amber mutation" codon usage, that is, the codon TAG was translated with the amino acid Gln. [c] Peptide IDs (**P1**, **P2**, **P3**, **P4**) are assigned to every sequence tested. [d] The value in brackets corresponds to the number of times the sequence was found to be repeated.

ry activity against *D. radiodurans* DXS. The peptides were dissolved in DMSO (for **P1** and **P2**) or water (for **P3** and **P4**) and their inhibitory activities against *D. radiodurans* DXS were tested by using a coupled assay with *E. coli* IspC as the auxiliary enzyme by monitoring the disappearance of NADPH spectrophotometrically at $\lambda = 340$ nm.[29] So as not to miss out on potential slow binders, we investigated the influence of incubating the peptides with *D. radiodurans* DXS in Tris·HCl buffer (pH 7.6) for 30 h both at room temperature and at 4 °C. Given that the activity of the enzyme was unchanged in the presence of up to 3% of DMSO, we performed both the direct measurements and the incubation studies with 2.5% of DMSO.

We noticed that the peptides dissolved in DMSO gave better results if incubated at 4 °C, whereas peptides dissolved in water showed the maximum inhibition at room temperature. The best results were obtained for **P2** (50% inhibition at 1000 μm after incubation at 4 °C for 30 hours) and particularly **P3** (47% inhibition at 250 μm after incubation at room temperature for 30 h; Table 4). Both **P2** and **P3** contain two adjacent Ser residues in the sequence: this Ser–Ser motif might function as a fingerprint for the recognition of the ThDP-binding pocket of *D. radiodurans* DXS. We performed a second round of phage display selection protocol by adding a custom-made library taking into account the Ser–Ser motif (see the Experimental Section for further details). After the selection, the eluted phages were sequenced, and the results are shown in Table 3. The list contains some sequences that were not present in the commercial library PhD12, such as A10, A06, A01, and D02, whereas A10 is a non-specific protein binder that we found several times in other displays.[35] A06 was repeated several times but did not have a Ser–Ser motif. The last two sequences (A01 and D02) might be contaminants given that they were

not repeated. Again, the selection did not result in the emergence of a particular motif, but rather in the enrichment of specific amino acids with some sequences occurring multiple times. As an example, **P9** was found several times, whereas others were not repeated but contained some recurring motifs such as the presence of additional Ser residues and multiple aromatic amino acids within the sequence (marked in bold and underlined in Table 3). Moreover, we observed that all the peptides contained at least one Pro residue, preferentially in the central part of the sequence, and a Leu or Ile residue, which might play a role in defining conformational preferences.

For ThDP-dependent enzymes such as TK, the binding pockets of ThDP and the acceptor substrate are often in proximity and even share some key amino acids[36–42] (Figure S3). This might also apply to DXS and its acceptor substrate, D-glyceraldehyde-3-phosphate (D-GAP). To identify both substrate- and cofactor-competitive inhibitors during screening, the concentrations of both ThDP and D-GAP should be adjusted accordingly upon evaluation of the inhibitory activity. *D. radiodurans* DXS does not afford satisfactory data quality under low concentrations of both D-GAP and ThDP. Thus, we proposed two rounds of activity evaluation, with assay conditions I and assay conditions II aimed at identifying ThDP- and D-GAP-competitive inhibitors, respectively (Table 4). We omitted preincubation upon screening for D-GAP-competitive inhibitors, as binding of this substrate is neither tight nor irreversible. The results of two rounds of activity evaluation of **P5**–**P12** against *D. radiodurans* DXS are summarized in Table 4. Peptide **P13** from the first phage display also contains the Ser–Ser motif; therefore, we tested its activity even though the sequence was not enriched.

During the inhibitory evaluation with assay conditions I, **P7** showed an IC$_{50}$ value of (13 ± 3) μm, and **P13** emerged as a double-digit micromolar inhibitor of *D. radiodurans* DXS [IC$_{50}$ = (49 ± 11) μm] after incubation at 4 °C for 30 hours. The other peptides did not show any inhibition or only very weak inhibitory activity (e.g., **P10**, 20% inhibition at 1000 μm). We determined the accurate concentration of **P7** in solution by UV spectrophotometry by taking advantage of the fact that **P7** contains a single Trp residue. As a consequence, the IC$_{50}$ value was recalculated to (9.5 ± 2.0) μm. Unfortunately, it was not possible to determine the accurate concentration of **P13** in solution by absorbance measurements owing to the absence of Trp or Tyr residues in the amino-acid sequence.

As for activity evaluation with assay conditions II, **P12**, the peptide found in eight phage clones after the second round of phage display, has an IC$_{50}$ value of (461 ± 25) μm. The difference in IC$_{50}$ values under the two screening conditions could be an indication that **P12** might be D-GAP-competitive. Peptide **P7** has an increased IC$_{50}$ value of (86 ± 13) μm; this indicates it might be ThDP competitive. Peptide **P13** did not exhibit any activity with assay conditions II, which suggests that it might indeed be slow binding and ThDP competitive or that preincubation might determine its activity.

The use of a coupled spectrophotometric assay requires a follow-up assay with the auxiliary enzyme IspC. Therefore, we

Table 3. Peptide sequences obtained after the round of second phage display.

Sequence ID	Sequence[a,b]	Peptide ID[c,d]
A01	KAIRTRGKRPQY	
A02	**Y**SSTI**Y**TPTAVG	**P5**
A03	GSSLL**Y**S**G**S**GPA	**P6**
A06	MAIPTRGKMPQY	**P12** (×8)
A10	ALWPPNLHAWVP[d]	
A11	**S**SSPVA**W**ALAMR	**P7**
B02	HSSPP**F**P**W**LLVT	**P10**
B07	DSS**S**G**L**YLRPL**S**	**P8**
B12	VSS**S**I**F**PIALPD	**P11**
C02	HSSPVQTD**W**ITV	**P9** (×4)
D02	THPSTKVPGTPA	
E05	ASSVI**S**PR**W**LL**W**	
E07	ALWPPNLHAWVP[d]	
F09	TSSAAAP**YYS**PP	
G05	VSSMKGPTL**S**TN	
H06	DSST**W**L**F**L**SS**YR	

[a] Peptide sequences were generated by translating the sequenced DNA considering the "amber mutation" codon usage, that is, the codon TAG was translated with the amino acid Gln. [b] Extra Ser residues and aromatic residues are in bold and underlined. [c] The value in brackets corresponds to the number of times the sequence was found to be repeated. [d] Indicates a contaminant sequence that nonspecifically recognizes any protein.

Table 4. List of peptides selected from the first and second phage displays and their inhibitory activities against *D. radiodurans* DXS, both in direct measurements and after incubation.

First round of phage display

Peptide ID[a]	Solvent[h]	Inhibition [%][b]
P1	DMSO	30 (at 1000 μM)[c]
P2	DMSO	50 (at 1000 μM)[c]
P3	H_2O	47 (at 250 μM)[c]
P4	H_2O	30 (at 1000 μM)[c]

Second round of phage display: Assay conditions I[e]

Peptide ID[a]	Solvent[h]	IC_{50} [μM]
P5	DMSO	>1000
P6	DMSO	>1000
P7	H_2O	13±3 (9.5±2.0)[d]
P8	H_2O	>500
P9	H_2O	>500
P10	DMSO	>1000
P11	DMSO	>1000
P12	H_2O	>1000
P13	DMSO	49±11[c]

Second round of phage display: Assay conditions II[f,g]

P5	DMSO	>1000
P6	DMSO	>1000
P7	DMSO	86±13
P8	DMSO	>500
P9	DMSO	>500
P10	DMSO	>1000
P11	DMSO	>1000
P12	DMSO	461±25
P13	DMSO	>1000

[a] P1–P4 are amidated at the C terminus; peptides P5–P13 are not amidated at the C terminus. [b] Percentage inhibition and IC_{50} values were determined by using a spectrophotometric assay. Full details of the biochemical assay conditions are provided in the Experimental Section. The values reported in the table correspond to the maximum concentration of the peptide soluble in the assay conditions. [c] Percentage of inhibition or IC_{50} values obtained after preincubation of the peptide in Tris·HCl buffer (pH 7.6) with *D. radiodurans* DXS for 30 h at room temperature and/or at 4 °C. [d] The value in parentheses corresponds to the recalculated IC_{50} value on the basis of the concentration of the peptide determined by absorbance, as described in the Experimental Section. [e] Activity evaluation with assay conditions I aimed at screening for ThDP competitive inhibitors, with 1.2 μM of ThDP, 10×K_m (ThDP), and 0.5 mM of D-GAP, 15×K_m (D-GAP). [f] Activity evaluation with assay conditions II aimed at screening for D-GAP competitive inhibitors, with 0.1 mM of ThDP, 0.1 mM of D-GAP, 3×K_m (D-GAP). [g] Preincubation was not performed in this round of evaluation, as substrate binding of DXS was considered to be neither tight nor irreversible. [h] DMSO concentration was 3%.

Table 5. Results of the detergent assay and DXS concentration dependence to identify false positives.

	Addition of detergent	DXS conc. [μM]	IC_{50} [μM]
P7[a]	–	0.4	13±3
	0.01% Triton X-100	0.4	>1000
	–	1.0	>1000
P13[a,c]	–	0.4	49±11
	0.01% Triton X-100[d]	0.4	>1000
	–	1.0	547±88
P12[b]	–	0.4	461±25
	0.01% Triton X-100	0.4	449±33
	–	1.0	472±16

[a] Assay conditions I were used for P7 and P13. [b] IC_{50} of P12 was determined with assay conditions II. [c] Preincubation was performed in all three assays of P13. [d] For P13, detergent was added after preincubation.

activity at different DXS concentrations (Table 5).[45] The results demonstrate that the addition of a small amount of detergent or an increase in the concentration of DXS led to significant attenuation of inhibitory activity for P7 and P13, whereas P12 was not affected. To corroborate this result, solutions of P7 and P13 in assay buffer were investigated by transmission electron microscopy (TEM), and the formation of fibers was observed (Figure S4). Taken together, three independent experiments showed that P7 and P13 are nonspecific inhibitors that inhibited DXS and IspC by aggregating into fibers and sequestering the enzyme.[46] Even though we used low-binding tubes during phage display and 0.05% Tween 20 in the washing buffer, it might not have been sufficient to exclude all of the false positives. Here, we showed that such fiber-forming nonspecific inhibitors could be conveniently identified by adding 0.01% Triton X-100 to the assay buffer. To the best of our knowledge, we report here for the first time the application of the detergent assay on peptidic inhibitors. Peptide P12 was confirmed as a true inhibitor against *D. radiodurans* DXS.

As it is not active against IspC, its MOI could be studied with the coupled assay. For substrate-competitive inhibitors, the Cheng–Prusoff Equation (1) holds:[47]

$$IC_{50} = K_i \left(\frac{1 + [S]}{K_m} \right) \tag{1}$$

in which [S] represents the concentration of the corresponding substrate, and K_m is the Michaelis–Menten constant in the absence of the inhibitor. By varying the initial substrate concentration and plotting IC_{50} against $(1+[S]/K_m)$, a competitive inhibitor should generate a straight line passing through the origin, with the slope equivalent to the inhibition constant, K_i.[48,49] The MOI study of P12 competing with D-GAP is shown in Figure 1.

The results of cofactor and pyruvate competition are shown in Figure S5.

The full kinetic characterization revealed that P12 is a D-GAP-competitive inhibitor, with $K_i = (113 \pm 4)$ μM, and noncompetitive with respect to both the cofactor ThDP and the donor substrate pyruvate.

tested P7 for its inhibitory potency against *E. coli* IspC and found that it has an IC_{50} value of (490 ± 60) μM. Peptide P13 is not active against *E. coli* IspC without preincubation but shows an IC_{50} value of (266 ± 42) μM after preincubation. Peptide P12 is not active against IspC.

Although DXS and IspC catalyze the first two reactions of the MEP pathway, their structures and functions are very different. The fact that P7 and P13 inhibits both enzymes raised our concern of nonspecific inhibition. To eliminate false-positive peptides before the MOI study, we performed a detergent assay, which is commonly used to confirm small-molecule aggregators.[43,44]

In parallel, given that inhibition arising from aggregation depends on the amount of enzyme, we compared the inhibitory

Figure 1. Mode-of-inhibition study of **P12**. Peptide **P12** is competitive with acceptor-substrate D-GAP, as illustrated by linearity between the XY series.

As **P12** was washed out using a ThDP buffer, this result validated our previous hypothesis: for DXS, and some other ThDP-dependent enzymes, the binding pockets of ThDP and the acceptor substrate are closely related, both structurally and functionally, and may not be considered completely separately.

Different from our expectations, we did not identify any ThDP-competitive peptidic inhibitor during the second round of phage display. A possible reason might be that the stringent phage library coincidentally did not contain any hits. Furthermore, the polar character of the diphosphate-binding pocket together with the possibility for metal chelation make the identification of ThDP-competitive inhibitors through phage display challenging.

Conclusions

Herein, we reported the discovery of a D-GAP-competitive peptidic inhibitor, **P12**, with a K_i value of (113 ± 4) μM, by phage display targeting the thiamine diphosphate (ThDP)-binding pocket. The expected ThDP-competitive inhibitors were confirmed to be nonspecific false positives by using the detergent assay and transmission electron microscopy. Similar to what was found for other ThDP-dependent enzymes, our results indicate that the cofactor- and acceptor-substrate-binding pockets are closely related both structurally and functionally. This property might provide inspiration to design novel inhibitors for 1-deoxy-D-xylulose-5-phosphate synthase (DXS), targeting the key amino acids shared by the ThDP- and D-GAP-binding pockets. Peptide **P12** is the first known peptidic inhibitor of DXS and sets the stage for further rounds of optimization.

Experimental Section

Bacterial strain: *E. coli* ER2738 (NEB E4104S) [Genotype: F′*proA*⁺*B*⁺ *lacI*�q *Δ(lacZ)M15 zzf::Tn10*(TetR)/ *fhuA2 glnV Δ(lac-proAB) thi-1 Δ(hsdS-mcrB)5*] is a male *E. coli* in which F′ can be selected for by using tetracycline, and it allows Blue/White screening and is an amber mutant strain. It was used for cloning and expression of the phage library, for titering, and for inoculation of the sequencing plates.

Phage display I: The first phage-display selection protocol was performed by using the commercially available M13 library PhD12 (NEB E8111L) consisting of M13 phages expressing a 12aa peptide

at the N terminus of each coat protein p3, and a small Gly–Gly–Gly–Ser linker was inserted between the peptide and the coat protein to increase the conformational freedom of the exposed peptides and to minimize the contribution of the protein p3 to the overall binding. The schematic sequence of this library is *N*-term-X₁₂-GGGS-p3-C-term. Three rounds of selection were performed in phosphate-buffered saline (PBS; 1 mL, sodium phosphate 50 mM, NaCl 150 mM, pH 7.5) incubating 10E10 phages with *D. radiodurans* DXS (1 mg) in a 2 mL protein-low-binding tube for 30 min on ice. For the first two rounds, DXS functionalized with *N*-hydroxysuccinimide (NHS)–desthiobiotin and Dynabeads MyOne Streptavidin C1 (Invitrogen 65001) were used to capture DXS from the solution. For the third round, to avoid selection of phages against streptavidin and given that *D. radiodurans* DXS contains an N-terminal His-tag, MagneHis Ni Particles (Promega V8560) were used as capturing system. After the incubation step, 0.1 mL of beads were added to the solution, which was mixed in a thermo shaker at 4 °C for 15 min. The tube was placed in a magnetic rack to allow for adhesion of the magnetic beads on one side of the tube. Phages expressing DXS binders were retained on the bead surface, and the buffer containing unbound phages was gently discarded from the tube. To remove weakly bound phages further, the beads were washed with PBST (10×1 mL PBS with 0.05 % Tween 20) whilst retaining them using a magnetic rack. The elution of strongly bound phages from the beads was achieved by suspending the beads in the elution buffer (1 mL, 1 mM Biotin in PBS for rounds 1 and 2 and 500 μM imidazole in PBS for round 3). After separation of the beads, the solution containing the eluted phages was used to amplify the selected pool of phages by infecting a fresh culture of *E. coli* ER2738. Infection, production, and purification of the phages were performed by following the manufacturer's manual. Peptides **P1**–**P4** were purchased from CASLO (Lyngby, Denmark) with purity >97 % according to HPLC.

Library design and cloning: A custom-made library was designed to include the motif Ser–Ser at the N terminus of the peptide library. Two oligomers, one coding for the library itself and one used for cloning purposes were designed:

Library oligo: CATGT TTCGG CCGA(MNN)₉ GGAGG AMNNA GAGTG AGAAT AGAAA GGTAC CCGGG

Extension primer: CATGC CCGGG TACCT TTCTA TTCTC

The "library primer" codes for the reverse strand of the library, and it includes two flanking regions that contain the restriction site for KpnI/Acc651 and EagI needed for cloning into the M13KE vector. The random part of the peptide sequence is coded by NNK codons (reverse complement of MNN), for which N is any of the bases, whereas K represents G or T (thus, M represents C or A). An NNK codon can encode for all 20 amino acids but only for one stop-codon: TAG. Combining the use of NNK codons with amber mutant strains such as *E. coli* ER2738 ensures that the whole library will code for full-length peptides. The "extension primer" is partially complementary with the library-coding oligomer, and it was used to generate the double-stranded DNA needed for cloning. The preparations of the library duplex and the cloning were performed as indicated in the manufacturer's manual (NEB E8111L).

Phage display II: Two rounds of selection were performed by using a custom-made phage library. The schematic sequence of the expressed library is: N-term-XSSX9-GGGS-p3-C-term. TBS (tris-buffered saline, 50 mM Tris·HCl pH 7.5, 150 mM NaCl) was used as incubation buffer, TBST (TBS with 0.05 % Tween 20) was used as washing buffer, MagneHis Ni Particles (Promega V8560) were employed for protein recovery, and 1 mM ThDP in TBS was used as

elution buffer. ThDP was chosen as competitive eluent to elute peptides specifically interacting with the ThDP-binding site of DXS. The same procedure as described for phage display I was used with the following modifications: DXS (1 mg) was incubated simultaneously with phages from the new library, phages from the original PhD-12 library were added to increase sequence complexity, and wild-type phages were supplemented to screen for nonspecific binders. The different phage pools were mixed in a 1:1:1 ratio prior to incubation with the target.

Sequencing: The last elution fractions from the phage display experiments were serially diluted (1:10) and used to infect a fresh culture of *E. coli* ER2738. The infected culture was plated on lysogeny broth (LB)–agar supplemented with tetracycline, isopropyl β-D-1-thiogalactopyranoside (IPTG), and XGal. Blue colonies resulting from phage infection were picked and sent for Sanger sequencing (at GATC Biotech) by using a custom-designed M13-specific sequencing primer (GTACA AACTA CAACG CCTGT). Peptides **P5**–**P13** and **P7a**–**P7l** were purchased from ProteoGenix SAS (Schiltigheim, France) with purity > 95% according to HPLC.

Gene expression and protein purification of *D. radiodurans* DXS: Gene expression and protein purification of *D. radiodurans* DXS were performed as reported in the literature.[13]

Spectrophotometric assay for determination of IC_{50} values against *D. radiodurans* DXS (assay conditions I): Direct measurements of the inhibitory activities with the spectrophotometric assay were performed as reported previously.[13] The tolerance of DXS with respect to DMSO concentration was determined by measurement of the reaction velocity in the presence of different concentrations of DMSO. The activity of the enzyme was found to be stable in the presence of up to 3% DMSO. To determine the inhibitory activity of the peptides after incubation, several solutions were prepared containing degassed Tris·HCl (pH 7.6, 100 mM. 300 µL), *D. radiodurans* DXS (0.79 µM), and different concentrations of each peptide with a dilution factor of 1:2 starting, if possible, from 1000 µM. The solutions were incubated at room temperature or at 4 °C for 30 h. Preliminary control experiments showed that the activity of *D. radiodurans* DXS was unchanged at room temperature or at 4 °C after 30 h. After the incubation time, each incubated solution (95 µL) was transferred to a 96-well plate, and a buffer containing Tris·HCl (pH 7.6, 100 mM) and D-glyceraldehyde-3-phosphate (4.0 mM) was added (47.5 µL). The reaction was started by the addition of a buffer solution (47.5 µL) containing Tris·HCl (pH 7.6, 100 mM), $MnCl_2$ (16 mM), dithiothreitol (DTT, 20 mM), NADPH (2.0 mM), sodium pyruvate (2.0 mM), ThDP (4.89 µM), and *E. coli* IspC (8.2 µM). A control experiment with the enzyme incubated in Tris·HCl buffer (and DMSO if testing peptides as stock solutions in DMSO) at the same temperature and for the same time was performed in parallel to monitor for potential loss in activity of the enzyme itself, which has never been observed. The reaction was monitored photometrically at room temperature at $\lambda = $ 340 nm by using a Synergy Mx (Biotek) microplate reader. Absorbance readings were taken every 30 s.

Spectrophotometric assay for determination of IC_{50} values against *D. radiodurans* DXS (assay conditions II): Photometric assays were conducted in transparent flat-bottomed 384-well plates (Nunc MaxiSorp). Assay mixtures contained Tris·HCl (100 mM, pH 7.6), 4 mM $MnCl_2$, dithiothreitol (DTT; 2 mM), 0.5 mM NADPH, 15 µM ThDP, 1.0 mM sodium pyruvate, 0.1 mM glyceraldehyde-3-phosphate, 8.3 µM *E. coli* IspC, 0.4 µM *D. radiodurans* DXS, and 3% DMSO. Buffer A contained Tris·HCl (100 mM, pH 7.6), 8 mM $MnCl_2$, DTT (4 mM), 1 mM NADPH, and 30 µM ThDP. Buffer B con-

tained Tris·HCl (100 mM, pH 7.6), 2.0 mM sodium pyruvate, and 0.2 mM glyceraldehyde-3-phosphate. The dilution series was performed in DMSO (2.4 µL) in each well, starting with a 80 mM DMSO stock solution of **P12** and covered the concentration range of 2000 to 2.0 µM. The reaction was started by adding buffer A (30 µL) to buffer B (30 µL). The reaction was monitored photometrically at room temperature at $\lambda = $ 340 nm by using a Synergy H1 (Biotek) microplate reader. Initial rate values were evaluated with a nonlinear regression method by using the program Dynafit.[50]

MOI study: Photometric assays were conducted in transparent flat-bottomed 384-well plates (Nunc MaxiSorp). Michaelis–Menten constants of cofactor and both substrates were determined with a previously reported method.[48,49] IC_{50} values were determined under assay conditions II, with variation of cofactor and substrates, respectively. The result was repeated in duplicate. The K_i value was calculated with SigmaPlot 13.

Gene expression, purification of *E. coli* IspC, and biochemical evaluation of inhibitory activity against *E. coli* IspC by spectrophotometric assay: Gene expression and purification of *E. coli* IspC were performed according to a literature procedure.[51] 1-Deoxy-D-xylulose-5-phosphate reductoisomerase (IspC) of *E. coli* bearing a His_6-tag at its N-terminal end was produced in and purified from recombinant *E. coli* strain M15 pQEYAEM. Cells were grown in LB medium in a shaker at 37 °C supplied with ampicillin (100 mg mL^{-1}) until the OD_{600} value reached 0.4. Thereafter, IPTG was added to a final concentration of 1 mM, and the cell suspension was incubated further at 30 °C with vigorous agitation for 16 h. Thereafter, cells were harvested by centrifugation, washed once with 0.9% NaCl solution, and frozen at −20 °C for storage.

For DXR purification, cell paste (5 g) was resuspended in Tris hydrochloride buffer (25 mL, 50 mM, pH 8.0), NaCl (300 mM), 0.02% NaN_3, and 15% imidazole and disrupted in French Press; cell debris was centrifuged down, and the supernatant was placed on the top of a Ni-NTA column (1×10 cm). After unbound proteins were washed from the column with the same buffer, the column was developed with an imidazole gradient (15–800 mM). Eluent fractions containing DXS were identified with SDS-polyacrylamide gel electrophoresis, combined, dialyzed versus Tris hydrochloride (30 mM, pH 8.0), 30 mM NaCl, 1 mM DTT, and 0.02% NaN_3 and concentrated by ultrafiltration and frozen at −80 °C for storage.

Spectrophotometric assay for determination of IC_{50} values against *E. coli* IspC: Biochemical evaluation of the inhibitory activity of **P7** against *E. coli* IspC was performed according to a protocol reported in the literature.[52] Spectrophotometric inhibition assays with *E. coli* IspC were performed in 384-well plates with a flat transparent bottom. Assay mixtures (total volume: 60 mL) contained Tris hydrochloride (100 mM, pH 7.6), 4 mM $MnCl_2$, 5 mM DTT, 0.5 mM NADPH, 5% DMSO, 30 nM of recombinant IspC protein, and tested compound. Dilution series (1:3) of potential inhibitors covered the concentration range of 200 to 0.2 µM. The reaction was started by the addition of 1-deoxyxylulose-5-phosphate (DXP) to a final concentration of 0.5 mM. The reaction was monitored photometrically ($\lambda = $ 340 nm) at room temperature (20–23 °C) in a microplate reader (SpectraMax M5, Molecular Devices, USA). Initial rate values were evaluated by using the nonlinear regression method with the program Dynafit.[50]

Conflict of Interest

The authors declare no conflict of interest.

[1] World Health Organization, *Global Tuberculosis Control: WHO report*, **2017** http://www.who.int/tb/publications/global_report/en/.

[2] World Health Organization, *World Malaria Report 2017*, **2017** http://www.who.int/malaria/publications/world-malaria-report-2017/en/.

[3] C. Wongsrichanalai, J. K. Varma, J. J. Juliano, M. E. Kimerling, J. R. MacArthur, *Emerging Infect. Dis.* **2010**, *16*, 1063 – 1067.

[4] T. Masini, A. K. H. Hirsch, *J. Med. Chem.* **2014**, *57*, 9740 – 9763.

[5] A. C. Brown, T. Parish, *BMC Microbiol.* **2008**, *8*, 78.

[6] A. R. Odom, W. C. Van Voorhis, *Mol. Biochem. Parasitol.* **2010**, *170*, 108 – 111.

[7] M. Rohmer, *Nat. Prod. Rep.* **1999**, *16*, 565 – 574.

[8] D. Arigoni, S. Sagner, C. Latzel, W. Eisenreich, A. Bacher, M. H. Zenk, *Proc. Natl. Acad. Sci. USA* **1997**, *94*, 10600 – 10605.

[9] F. Lynen, *Pure Appl. Chem.* **1967**, *14*, 137.

[10] J. Marcos, P. Rodriguez Russo, S. Lima, E. L. Rodriguez, *J. Clin. Rheumatol.* **2004**, *10*, 21 – 24.

[11] W. N. Hunter, *J. Biol. Chem.* **2007**, *282*, 21573 – 21577.

[12] http://clinicaltrials.gov/show/NCT02198807, retrieved 1.12.2017.

[13] T. Masini, J. Pilger, B. S. Kroezen, B. Illarionov, P. Lottmann, M. Fischer, C. Griesinger, A. K. H. Hirsch, *Chem. Sci.* **2014**, *5*, 3543 – 3551.

[14] S. Xiang, G. Usunow, G. Lange, M. Busch, L. Tong, *J. Biol. Chem.* **2007**, *282*, 2676 – 2682.

[15] L. A. Brammer, J. M. Smith, H. Wade, C. F. Meyers, *J. Biol. Chem.* **2011**, *286*, 36522 – 36531.

[16] R. Kluger, K. Tittmann, *Chem. Rev.* **2008**, *108*, 1797 – 1833.

[17] R. E. Hill, K. Himmeldirk, I. A. Kennedy, R. M. Pauloski, B. G. Sayer, E. Wolf, I. D. Spenser, *J. Biol. Chem.* **1996**, *271*, 30426 – 30435.

[18] Q. Du, H. Wang, J. Xie, *Int. J. Biol. Sci.* **2011**, *7*, 41 – 52.

[19] V. K. Singh, I. Ghosh, *FEBS Lett.* **2013**, *587*, 2806 – 2817.

[20] T. Masini, B. Lacy, L. Monjas, D. Hawksley, A. R. de Voogd, B. Illarionov, A. Iqbal, F. J. Leeper, M. Fischer, M. Kontoyianni, A. K. Hirsch, *Org. Biomol. Chem.* **2015**, *13*, 11263 – 11277.

[21] C. Mueller, J. Schwender, J. Zeidler, H. K. Lichtenthaler, *Biochem. Soc. Trans.* **2000**, *28*, 792 – 793.

[22] Y. Matsue, H. Mizuno, T. Tomita, T. Asami, M. Nishiyama, T. Kuzuyama, *J. Antibiot.* **2010**, *63*, 583 – 588.

[23] B. Altincicek, M. Hintz, S. Sanderbrand, J. Wiesner, E. Beck, H. Jomaa, *FEMS Microbiol. Lett.* **2000**, *190*, 329 – 333.

[24] J. Mao, H. Eoh, R. He, Y. Wang, B. Wan, S. G. Franzblau, D. C. Crick, A. P. Kozikowski, *Bioorg. Med. Chem. Lett.* **2008**, *18*, 5320 – 5323.

[25] J. M. Smith, R. J. Vierling, C. F. Meyers, *MedChemComm* **2012**, *3*, 65 – 67.

[26] J. M. Smith, N. V. Warrington, R. J. Vierling, M. L. Kuhn, W. F. Anderson, A. T. Koppisch, C. L. Freel Meyers, *J. Antibiot.* **2014**, *67*, 77 – 83.

[27] P. Vlieghe, V. Lisowski, J. Martinez, M. Khrestchatisky, *Drug Discovery Today* **2010**, *15*, 40 – 56.

[28] R. Hyde-DeRuyscher, L. A. Paige, D. J. Christensen, N. Hyde-DeRuyscher, A. Lim, Z. L. Fredericks, J. Kranz, P. Gallant, J. Zhang, S. M. Rocklage, D. M. Fowlkes, P. A. Wendler, P. T. Hamilton, *Chem. Biol.* **2000**, *7*, 17 – 25.

[29] P. M. Glee, S. H. Pincus, D. K. McNamer, M. J. Smith, J. B. Burritt, J. E. Cutler, *J. Immunol.* **1999**, *163*, 826 – 833.

[30] J. Li, C. Zhang, X. Xu, J. Wang, H. Yu, R. Lai, W. Gong, *FASEB J.* **2007**, *21*, 2466 – 2473.

[31] M. W. Peczuh, A. D. Hamilton, *Chem. Rev.* **2000**, *100*, 2479 – 2494.

[32] A. A. Thomas, J. De Meese, Y. Le Huerou, S. A. Boyd, T. T. Romoff, S. S. Gonzales, I. Gunawardana, T. Kaplan, F. Sullivan, K. Condroski, J. P. Lyssikatos, T. D. Aicher, J. Ballard, B. Bernat, W. DeWolf, M. Han, C. Lemieux, D. Smith, S. Weiler, S. K. Wright, G. Vigers, B. Brandhuber, *Bioorg. Med. Chem. Lett.* **2008**, *18*, 509 – 512.

[33] N. Nemeria, Y. Yan, Z. Zhang, A. M. Brown, P. Arjunan, W. Furey, J. R. Guest, F. Jordan, *J. Biol. Chem.* **2001**, *276*, 45969 – 45978.

[34] G. P. Smith, *Science* **1985**, *228*, 1315 – 1317.

[35] A. Marcozzi, R. Groningen, *Harnessing Phages for Supramolecular and Materials Chemistry*, University of Groningen, **2016**.

[36] P. Asztalos, C. Parthier, R. Golbik, M. Kleinschmidt, G. Hubner, M. S. Weiss, R. Friedemann, G. Wille, K. Tittmann, *Biochemistry* **2007**, *46*, 12037 – 12052.

[37] L.-J. Hsu, N.-S. Hsu, Y.-L. Wang, C.-J. Wu, T.-L. Li, *Protein Eng. Des. Sel.* **2016**, *29*, 513 – 522.

[38] S. Lüdtke, P. Neumann, K. M. Erixon, F. Leeper, R. Kluger, R. Ficner, K. Tittmann, *Nat. Chem.* **2013**, *5*, 762 – 767.

[39] L. Mitschke, C. Parthier, K. Schroder-Tittmann, J. Coy, S. Ludtke, K. Tittmann, *J. Biol. Chem.* **2010**, *285*, 31559 – 31570.

[40] U. Nilsson, L. Meshalkina, Y. Lindqvist, G. Schneider, *J. Biol. Chem.* **1997**, *272*, 1864 – 1869.

[41] B. Nocek, M. Makowska-Grzyska, N. Maltseva, A. Joachimiak, W. Anderson, http://www.rcsb.org/pdb/explore/explore.do?structureId = 3M6L, **2010**.

[42] B. Nocek, M. Makowska-Grzyska, N. Maltseva, W. Anderson, A. Joachimiak, http://www.rcsb.org/pdb/explore/explore.do?structureId = 3M7I, **2010**.

[43] B. Y. Feng, B. K. Shoichet, *Nat. Protoc.* **2006**, *1*, 550 – 553.

[44] B. K. Shoichet, *Drug Discovery Today* **2006**, *11*, 607 – 615.

[45] B. K. Shoichet, *J. Med. Chem.* **2006**, *49*, 7274 – 7277.

[46] M. Vodnik, U. Zager, B. Strukelj, M. Lunder, *Molecules* **2011**, *16*, 790 – 817.

[47] C. Yung-Chi, W. H. Prusoff, *Biochem. Pharmacol.* **1973**, *22*, 3099 – 3108.

[48] A. Ma, W. Yu, F. Li, R. M. Bleich, J. M. Herold, K. V. Butler, J. L. Norris, V. Korboukh, A. Tripathy, W. P. Janzen, C. H. Arrowsmith, S. V. Frye, M. Vedadi, P. J. Brown, J. Jin, *J. Med. Chem.* **2014**, *57*, 6822 – 6833.

[49] S. Apparsundaram, D. J. Stockdale, R. A. Henningsen, M. E. Milla, R. S. Martin, *J. Pharmacol. Exp. Ther.* **2008**, *327*, 982 – 990.

[50] P. Kuzmic, *Anal. Biochem.* **1996**, *237*, 260 – 273.

[51] S. Hecht, J. Wungsintaweekul, F. Rohdich, K. Kis, T. Radykewicz, C. A. Schuhr, W. Eisenreich, G. Richter, A. Bacher, *J. Org. Chem.* **2001**, *66*, 7770 – 7775.

[52] A. Kunfermann, C. Lienau, B. Illarionov, J. Held, T. Grawert, C. T. Behrendt, P. Werner, S. Hahn, W. Eisenreich, U. Riederer, B. Mordmuller, A. Bacher, M. Fischer, M. Groll, T. Kurz, *J. Med. Chem.* **2013**, *56*, 8151 – 8162.